



# The effects of temperature and reaction time on the formation of manganese ferrite nanoparticles synthesized by hydrothermal method

Oznur Karaagac<sup>1</sup> · Hakan Köçkar<sup>1</sup>

Received: 1 October 2019 / Accepted: 20 December 2019 / Published online: 1 January 2020  
© Springer Science+Business Media, LLC, part of Springer Nature 2020

## Abstract

In order to optimize the hydrothermally synthesized manganese ferrite nanoparticles, the nanoparticles were synthesized under different reaction conditions. The effects of reaction temperature and time were investigated in a wide range. The samples have additional phases (hematite, maghemite) at high temperatures, and the sample synthesized at 120 °C has two different types of nanoparticles. However, the pure manganese ferrite phase was obtained as the reaction time increased at 130 °C. Particle size increased from  $16.1 \pm 6.1$  nm to  $25.8 \pm 7.4$  nm and from  $19.4 \pm 8.4$  nm to  $25.8 \pm 8.2$  nm with the rise of reaction temperature and time, respectively. The saturation magnetization  $M_s$  of the nanoparticles also increased with the increase of reaction temperature and time. Although the  $M_s$  values and particle sizes are very close for the samples synthesized at high temperature (at 220 °C for 4 h) and long reaction time (16 h at 130 °C), pure phase of manganese ferrite with high  $M_s$  (65 emu/g) was observed at low temperature and long reaction time.

## 1 Introduction

Ferrites receive interest due to their unique properties. They have potential to be used in many areas (electronic devices, magnetic resonance imaging (MRI), magnetic hyperthermia, etc.). Among all ferrites, manganese ferrite has high magnetic permeability and low losses. It is a soft ferrite with a moderate saturation magnetization (80 emu/g) at room temperature [1]. Manganese ferrite is almost, but not perfectly, spinel; since in most cases, 80% of  $Mn^{2+}$  ions occupy tetrahedral sites (A) and the left 20% of them occupy octahedral sites (B) instead of all  $Mn^{2+}$  ions located at tetrahedral sites [1]. Manganese ferrite has been of great interest for its remarkable magnetic properties accompanied by good chemical stability and mechanical hardness. It is suitable for many applications because of these properties. Recently, many studies exhibited data about the potential applications of manganese ferrite such as supercapacitors [2–4], sensors [5], catalysis [6], environmental remediation [7–9] and biosensing of contaminations [3]. Also, many studies have been

reported on the properties of the manganese ferrite nanoparticles for MRI [10–12] and magnetic hyperthermia [13, 14].

Manganese ferrite nanoparticles are synthesized with many techniques including hydrothermal synthesis [3, 7–10, 13], thermal decomposition [4, 15], co-precipitation [2, 16], reverse micelle [14, 17] and mechanosynthesis [18]. The most common technique to synthesize manganese ferrite nanoparticles is hydrothermal synthesis. This technique takes place at high temperature and does not need calcination step after the synthesis. Also, the synthesis parameters can be controlled in order to tailor the properties of the nanoparticles.

The hydrothermal synthesis takes place at high temperatures; thus, the samples show other phases (hematite) besides manganese ferrite (and/or  $Zn^{2+}$ -substituted manganese ferrite) in some studies in which the selected synthesis temperatures are quite high ( $\geq 180$  °C) [8, 13, 19]. Since secondary phase is observed under different synthesis conditions, the effects of the hydrothermal synthesis parameters should be studied to obtain pure manganese ferrite. The phases of the samples synthesized by other techniques [18, 20] were investigated in terms of pure manganese ferrite phase formation. In [18], the formation of manganese ferrite nanoparticles and the phases of the products obtained by mechanosynthesis under different synthesis conditions were investigated. Herranz et al. [20] studied the effects of

✉ Oznur Karaagac  
karaagac@balikesir.edu.tr

<sup>1</sup> Physics Department, Science and Literature Faculty, Balikesir University, Cagis, 10145 Balikesir, Turkey

the synthesis parameters on the morphology and phases of the products obtained by microemulsion and also gave the phases of the products obtained by co-precipitation and physical synthesis for comparison. As far as concerned, the synthesis parameter studies about the secondary phases of manganese ferrite nanoparticles obtained by hydrothermal method were not come across by now. Thus, in this work, hydrothermal synthesis conditions were investigated to obtain pure manganese ferrite nanoparticles. Manganese ferrite nanoparticles were synthesized by hydrothermal method in a wide range of temperature in order to obtain the proper synthesis temperature. The reaction time was also studied, and the synthesis conditions were optimized.

## 2 Experimental details

### 2.1 Synthesis of the nanoparticles

MnSO<sub>4</sub>·H<sub>2</sub>O (Merck, ≥ 98%), FeCl<sub>3</sub>·6H<sub>2</sub>O (Sigma Aldrich, ≥ 99%) and NH<sub>4</sub>OH (Merck, 25%) were used for the synthesis of manganese ferrite nanoparticles. A 250-ml two-necked round-bottom flask was used for the synthesis of the precursor. 15 mmol of MnSO<sub>4</sub>·H<sub>2</sub>O and 30 mmol of FeCl<sub>3</sub>·6H<sub>2</sub>O were dissolved in 50 ml deionized water to obtain the metal ion solution. In order to obtain the precursor, 50 ml of NH<sub>4</sub>OH solution was added to the metal ions solution under vigorous stirring at 1000 rpm and stirred for 10 min by a mechanical stirrer (Velp Sientifica). For the hydrothermal process, 15 ml of the precursor was transferred into the Teflon-lined stainless steel autoclave (45 ml). Sealed autoclave was transferred into an oven (Nüve FN 055) for the hydrothermal synthesis of the nanoparticles. In order to study the effect of reaction temperature, the temperature

was varied between 100 °C and 220 °C with a fixed reaction time of 4 h. And, the reaction time was varied from 1 to 16 h at 130 °C to investigate the effect of reaction time. After the reaction, the precipitates were washed three times with deionized water. The samples were then dried in an oven at 60 °C to obtain powders. The sample synthesized at 100 °C was labelled as S100 and the other samples were labelled accordingly, see Table 1. And, for the investigation of reaction time, the sample synthesized for 1 h is labelled as S1 and the other samples were labelled accordingly, see also Table 1.

### 2.2 Characterizations of the nanoparticles

Structural analysis of the samples was conducted by X-ray diffraction (XRD) technique using Phillips PANalytical's X'Pert PRO diffractometer and Fourier transform infrared (FTIR) spectroscopy using Perkin Elmer Spectrum Two model spectrometer. XRD patterns were obtained in the  $2\theta = 20^\circ - 80^\circ$  range by using CuK<sub>α</sub> radiation ( $\lambda = 0.15406$  nm). The average crystallite size was calculated from the well-known Scherrer equation [21] using a value of 0.9 for the constant K and carrying out the instrumental width correction. This constant K depends on the crystallite geometry and size distribution. In addition, we need to know the strain in the crystallites. Thus, the crystallite sizes from the Scherrer equation listed in Table 1 are only first-order estimates. FTIR spectrum of the samples was recorded between 370 and 4000 cm<sup>-1</sup> by using KBr pellets. Transmission electron microscope (TECNAI G2 F30 model) was used to determine the shape and size of the nanoparticles. Energy-dispersive X-ray (EDX) spectroscopy, which was integrated to TEM, was also employed to obtain the elemental content of the samples. Magnetic measurements were made by using

**Table 1** Synthesis conditions, elemental analysis results, particles sizes and magnetic properties of manganese ferrite nanoparticles

Sample	Reaction temp. (°C)	Reaction Time (h)	Mn/Fe	$d_{\text{XRD}}$ (nm)	$d_{\text{TEM}}$ (nm)	a (nm)	$M_s$ (emu/g)	$M_r$ (emu/g)	$H_c$ (Oe)	$H_s$ (Oe)
S100	100		0.42	19	16.1 ± 6.1	0.8471	35	1.6	22	15,303
S120	120		0.26	18	15.4 ± 10.7	0.8449	49	3.0	28	12,262
S130	130	4	0.22	19	16.5 ± 9.4	0.8450	57	3.5	29	10,042
S160	160		–	–	–	–	61	5.3	38	6908
S190	190		–	–	–	–	62	5.7	40	5082
S220	220		0.20	21	25.8 ± 7.4	0.8482	64	8.5	58	3883
S1		1	–	4	1.8 ± 0.5	0.8435	16	0.1	1	17,679
S2		2	0.35	21	19.4 ± 8.4	0.8462	47	2.8	26	12,561
S4 (S130)	130	4	0.22	19	16.5 ± 9.4	0.8450	57	35	29	10,042
S8		8	0.29	25	–	0.8472	58	5.1	40	8842
S12		12	–	–	–	–	59	5.7	46	8544
S16		16	0.37	27	25.8 ± 8.2	0.8477	65	6.6	48	7175

\*Not saturated at the applied magnetic field

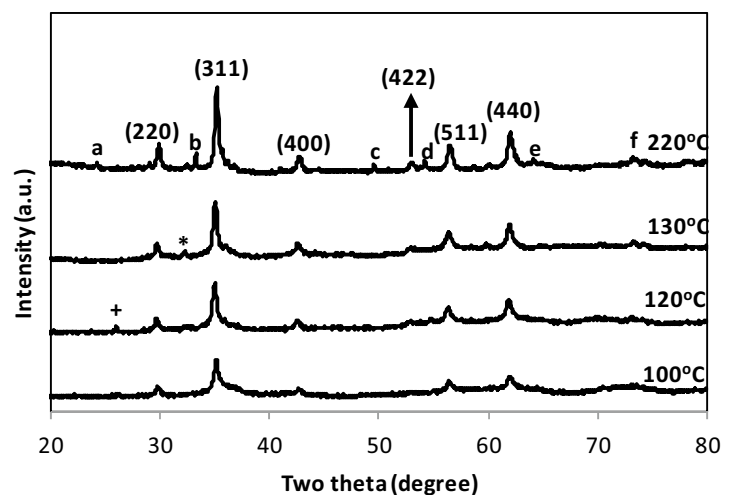
vibrating sample magnetometer (VSM, ADE EV 9 model) at room temperature with a maximum applied field of  $\pm 20$  kOe.

### 3 Results and discussion

In order to obtain pure manganese ferrite nanoparticles with high saturation magnetization, the nanoparticles were synthesized at different hydrothermal conditions. Reaction temperature and reaction time were investigated to optimize the nanoparticles. XRD patterns of the samples synthesized at different reaction temperatures (S100, S120, S130 and S220 were synthesized at 100°, 120°, 130° and 220 °C, respectively) are given in Fig. 1. Sample S100 has (220), (311), (400), (511) and (440) peaks of spinel manganese ferrite at around 29.9°, 35.2°, 42.7°, 56.4° and 62.0° according to the JCPDS card no. 10-0319. Other samples also have the same peaks of spinel manganese ferrite. Furthermore, (422) peak of spinel structure is also observed at around 53.0° in the XRD patterns of the samples synthesized at higher temperatures than 100 °C. Besides, sample S120 has a weak peak at around 26.1° which is indexed as the (211) peak of maghemite according to the JCPDS card no. 39-1346. Sample S130 also has a weak (221) peak of maghemite at around 32.2°. In the pattern of S220, the peaks of hematite are observed besides the peaks of manganese ferrite. The peaks around 24.3°, 33.3°, 49.6°, 54.1°, 64.1° and 72.3° are in accordance with the crystal planes of (012), (104), (024), (116), (300) and (119) of hematite (JCPDS card no. 33-0664). Furthermore, (110) and (214) peaks of hematite may be overlapped with the (311) and (440) peaks of manganese ferrite, respectively. The second phase is clearly observed in the XRD pattern of sample S220. XRD pattern of the sample S220 is consistent with the study of Cruz et al [13]. In the study, hematite phase was observed in the XRD patterns of

MnFe<sub>2</sub>O<sub>4</sub> nanoparticles that are hydrothermally synthesized at 230 °C. Thu et al [8] also showed that the sample synthesized at 180 °C had hematite phase. It is known that hematite can be obtained by hydrothermal synthesis at high temperatures (above 160 °C) [22–24]. Thus, in our study, the hematite phase is likely to be seen at higher synthesis temperatures ( $\geq 160$  °C) as indicated in other studies [8, 13]. EDX analysis of the samples was done and the results are given in Table 1. The Mn/Fe ratio of the samples S100, S120, S130 and S220 is 0.42, 0.22, 0.26 and 0.20, respectively. The Mn/Fe ratio of S100 is closer to stoichiometric ratio of 0.50. This is evidence that there is no secondary phase in the XRD pattern of sample S100. The Mn/Fe ratio decreases as the reaction temperature increases. The difference of the ratios from the stoichiometric ratio may be explained by the secondary phases (maghemite for sample S120 and S130 and hematite for sample S220) observed in the XRD patterns of the samples. The crystallite size  $d_{\text{XRD}}$  calculated by using the (311) peak of manganese ferrite for the samples S100, S120, S130 and S220 is 19 nm, 18 nm, 19 nm and 21 nm, respectively. The crystallite size of the samples increases as the reaction temperature increases as given in Table 1. The increase of the intensities of the peaks may be caused by the increase of the crystallite sizes, as well as the overlapping peaks of two phases. The lattice parameters were also calculated by using least squares technique and found to be 0.8471 nm, 0.8449 nm, 0.8450 nm and 0.8482 nm for the samples S100, S120, S130 and S220, respectively. The lattice parameters of the samples are in agreement with the lattice parameter of manganese ferrite (0.8499 nm) [25]. The decrease of lattice parameter in samples S120 and S130 may be caused by the maghemite phase which was observed in the XRD patterns of these samples since the lattice constant of maghemite is 0.8352 nm [26]. FTIR analysis was made for all samples and the spectra were given in the range of 370–4000 cm<sup>-1</sup> in Fig. 2. In the spectrum of S100 and S120, two peaks appear

**Fig. 1** XRD patterns of the nanoparticles synthesized at different temperatures. (Peaks of maghemite are indexed as +: (211) and \*: (221) and the peaks of hematite are indexed as (a) (012), (b) (104), (c) (024), (d) (116), (e) (300) and (f) (119))



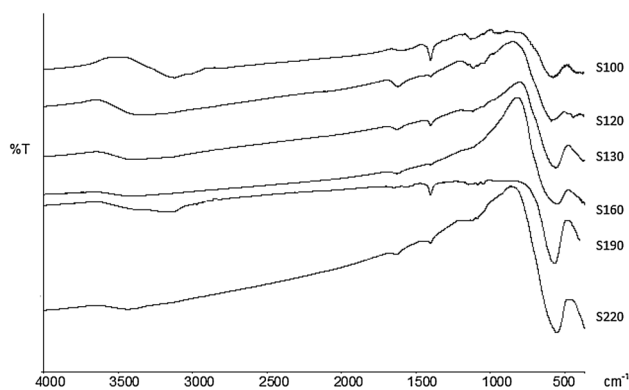


**Fig. 2** FTIR spectrum of the nanoparticles synthesized at different temperatures (S100: 100 °C, S120: 120 °C, S130: 130 °C, S160: 160 °C, S190: 190 °C and S220: 220 °C)

around  $400\text{ cm}^{-1}$  and  $580\text{ cm}^{-1}$  and correspond to the typical characteristic peaks of Mn–O and Fe–O bonds of manganese ferrite [17, 27]. As the reaction temperature increases, the peak around  $580\text{ cm}^{-1}$  sharpens and slightly shifts to lower values (towards  $550\text{ cm}^{-1}$ ). In some studies which include the synthesis of hematite at high temperatures, the peaks of hematite are observed at around  $525\text{ cm}^{-1}$  [24] and  $550\text{ cm}^{-1}$  [28]. By considering the current XRD analysis, it can be concluded that the shift of the peak at  $580\text{ cm}^{-1}$  towards lower values may be caused by the hematite phase. The stretching and vibration peaks of OH groups are also seen in FTIR spectra of the samples which indicate the OH groups on the surface of the nanoparticles as indicated in many studies [7, 8, 10]. Moreover, in the FTIR spectra of some samples, corresponding bands become weaker suggesting a reduction in the amount of OH groups [8].

TEM images of the manganese ferrite nanoparticles synthesized at different reaction temperatures are shown in Fig. 3. The calculated particle sizes are also presented in Table 1. The particle size  $d_{\text{TEM}}$  is  $16.1 \pm 6.1\text{ nm}$ ,  $15.4 \pm 10.7\text{ nm}$ ,  $16.5 \pm 9.4\text{ nm}$  and  $25.8 \pm 7.4\text{ nm}$  for the samples S100, S120, S130 and S220, respectively. The  $d_{\text{TEM}}$  is found to increase up to  $25.8 \pm 7.4\text{ nm}$  for the nanoparticles synthesized at 220 °C. These results are consistent with the XRD findings. High-resolution TEM (HRTEM) image of sample S100 is shown in Fig. 3b. The interplane spacing  $d$  was measured as  $0.312\text{ nm}$  from the image and the value corresponds to the (220) plane of manganese ferrite confirming the XRD results. In the TEM image of sample S120 (Fig. 3c), smaller nanoparticles are seen besides the bigger nanoparticles. As can be seen from the histogram, the sample consists of both 5–10 nm (smaller) and 25–30 nm (bigger) sized nanoparticles. Cruz et al [13] also found a similar bimodal size distribution in manganese ferrite nanoparticles synthesized at 175 and 230 °C. It is found from the EDX analysis that these different sized nanoparticles in sample

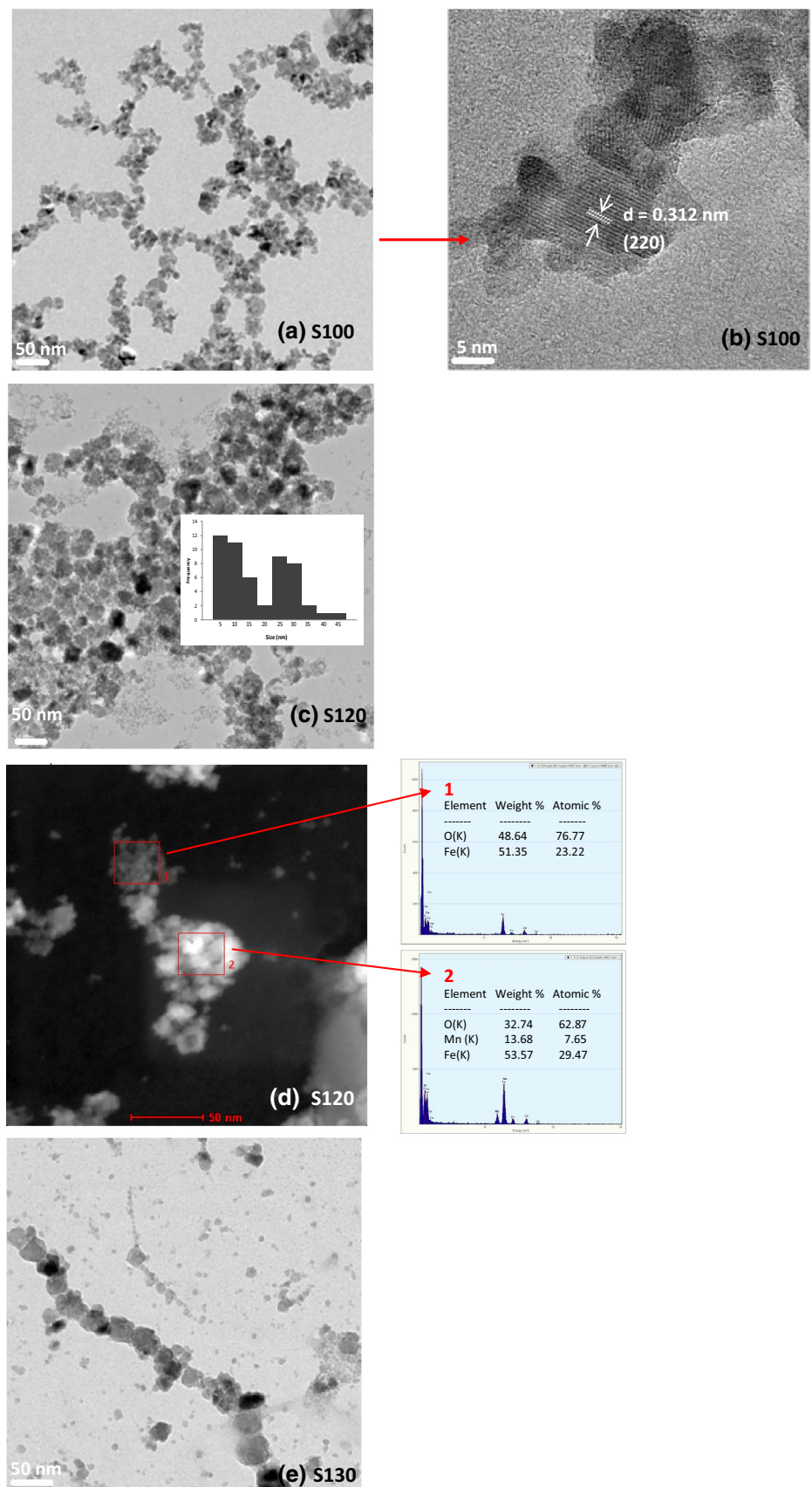
S120 also have different compositions. The high-angle annular dark-field (HAADF) image of the sample S120 is given in Fig. 3d with the EDX results of the selected nanoparticles. The bigger nanoparticles consist of at. %8 Mn, at. %29 Fe and at. %63 O; however, the smaller nanoparticles consist of at. %23 Fe and at. %77 O. It can be concluded that the sample has another phase besides manganese ferrite as presented in the XRD analysis of this sample.

Magnetic measurements of manganese ferrite nanoparticles were made by VSM at room temperature and the magnetization curves of the samples were given in Fig. 4 with insets (at the field range of  $\pm 750\text{ Oe}$ ). Saturation magnetization ( $M_s$ ), remenent magnetization ( $M_r$ ), coercivity ( $H_c$ ) and saturation field ( $H_s$ ) values of manganese ferrite nanoparticles can be seen in Table 1. The  $M_s$  of the samples increases from 35 to 64 emu/g and the  $H_c$  increases from 22 to 58 Oe with the increase of synthesis temperature from 100 to 220 °C.  $M_r$  values also increase from 1.6 to 8.5 emu/g as the reaction temperature increases. Besides, the  $H_s$  of the nanoparticles decrease with the increase of the reaction temperature indicating that it is easier to magnetize the nanoparticles synthesized at higher temperatures. The  $M_s$  of sample S220 (64 emu/g) is closer to the  $M_s$  of bulk manganese ferrite (80 emu/g) [1] despite the accompanying hematite phase whose  $M_s$  is as low as 0.4 emu/g [29].

Despite the high  $M_s$  observed at high reaction temperature, the sample (S220) consists of manganese and hematite phases. In order to obtain pure manganese ferrite nanoparticles with high  $M_s$ , the nanoparticles were synthesized at different reaction times at 130 °C. The XRD patterns of the nanoparticles synthesized at different times (S1, S2, S4 and S16) were given in Fig. 5. As can be seen from the pattern of S1, the only peak around  $35^\circ$ , which is indexed as (311) peak of manganese ferrite, is very weak and wide. The weak and wide peaks may indicate that the reaction does not completely take place or it may originate from small sized nanoparticles or poor crystallinity [30]. As the reaction time increases, the characteristic peaks of manganese ferrite noticeably appear. In the patterns of S2, S4 and S16, the peaks observed around  $29.9^\circ$ ,  $35.1^\circ$ ,  $42.7^\circ$ ,  $53.0^\circ$ ,  $56.5^\circ$  and  $62.0^\circ$  correspond to (220), (311), (400), (422), (511) and (440) crystal planes of spinel manganese ferrite (JCPDS card No. 10-0319), respectively. In the pattern of S2, there are two additional peaks at  $32.2^\circ$  and  $36.1^\circ$ . While the peak at lower angle indicates the (221) peak of maghemite (JCPDS card No. 39-1346), the one at higher angle may refer to either the (040) peak of goethite (JCPDS card. No. 81-0464) or the (111) peak of wüstite (JCPDS card No. 06-0615). In the XRD pattern of S4, only maghemite peak can be observed. As the reaction time increases, the additional peaks disappear as seen in the pattern of S16 and only manganese ferrite phase is observed.  $d_{\text{XRD}}$  values of the samples are calculated and given in Table 1.  $d_{\text{XRD}}$  of samples S1, S2, S4, S8 and



**Fig. 3** **a** TEM image of the nanoparticles synthesized at 100 °C, **b** HRTEM image of the sample S100 (the nanoparticles synthesized at 100 °C), **c** TEM image and histogram of the nanoparticles synthesized at 120 °C, **d** HAADF image and elemental analysis results of the nanoparticles synthesized at 120 °C and **e** TEM image of the nanoparticles synthesized at 130 °C



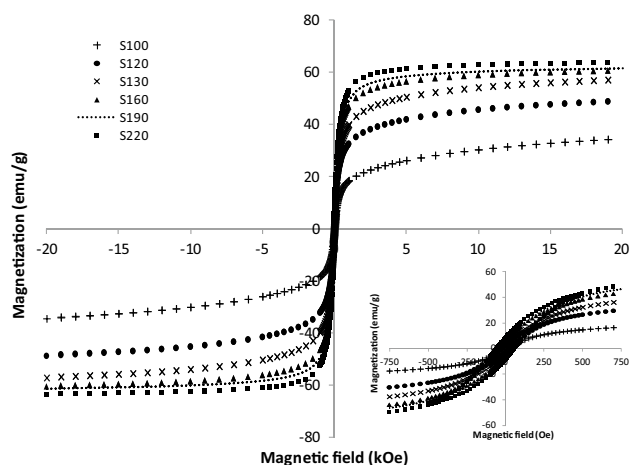


**Fig. 4** Magnetization curves of the nanoparticles synthesized at different temperatures (Inset shows the curves at  $\pm 750$  Oe.)

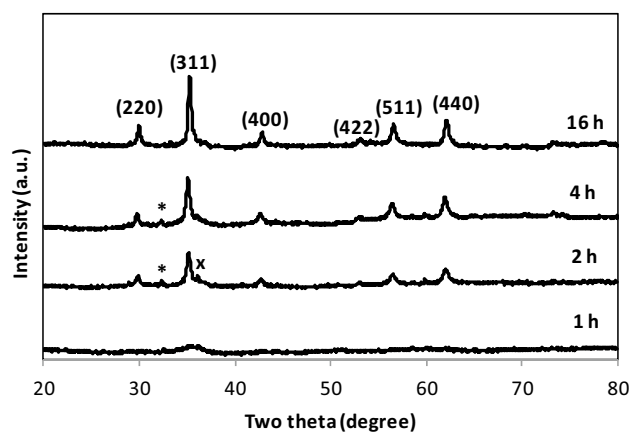


**Fig. 5** XRD patterns of manganese ferrite nanoparticles synthesized at different reaction times (\*shows the (221) peak of maghemite and \* shows the (040) peak of goethite or (111) peak of wüstite)

S16 is 4 nm, 21 nm, 19 nm, 25 nm and 27 nm, respectively. Peak intensities are seen to increase with the increase of reaction time due to the increase of particle size and crystallinity. With hydrothermal synthesis, it is shown that the reaction temperature and time affect the size and crystallinity of the nanoparticles [31]. The lattice parameters of the samples S1, S2, S4, S8 and S16 are also calculated and are given in Table 1. As the reaction time increases from 1 to 16 h, the lattice parameter increases from 0.8435 nm to 0.8472 nm and comes closer to the value of bulk manganese ferrite (0.8499 nm) [25]. FTIR spectrum of the samples synthesized at different reaction times are given in Fig. 6. The transmittance band seen around  $570\text{ cm}^{-1}$  indicates that all samples are manganese ferrite. However, the intensity of the peak in the spectrum of S1 is very low. The peak intensifies with the increase of the reaction time.

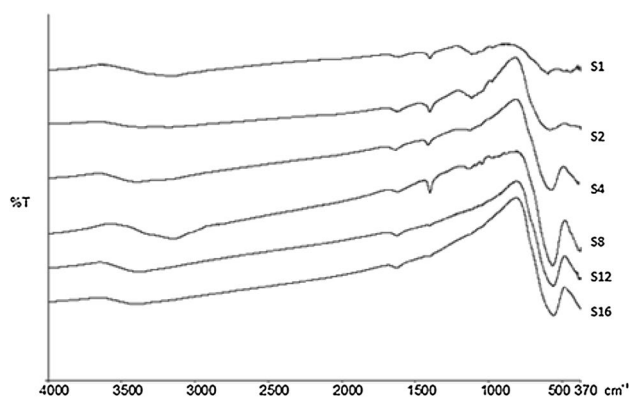


**Fig. 6** FTIR spectrum of the samples synthesized at different reaction times (S1: 1 h, S2: 2 h, S4: 4 h, S8: 8 h, S12: 12 h and S16: 16 h)

TEM images of the samples S1, S2 and S16 are given in Fig. 7a–c, respectively. As can be seen from the image of S1, the nanoparticles are very small in size ( $1.8 \pm 0.5$  nm) indicating the nucleation occurs; however, the reaction is not completed in 1 h.  $d_{\text{TEM}}$  of the samples is given in Table 1. It can be said that the reaction is more likely to be completed as the reaction time increases to 2 h since the particle size increases to  $19.4 \pm 8.4$  nm for sample S2. However, the XRD pattern of the sample S2 has secondary minor phase peaks; thus, the complete reaction may need longer time than 2 h. The particle size increases for the time being as the reaction time increases and reaches to  $25.8 \pm 8.2$  nm for sample S16.

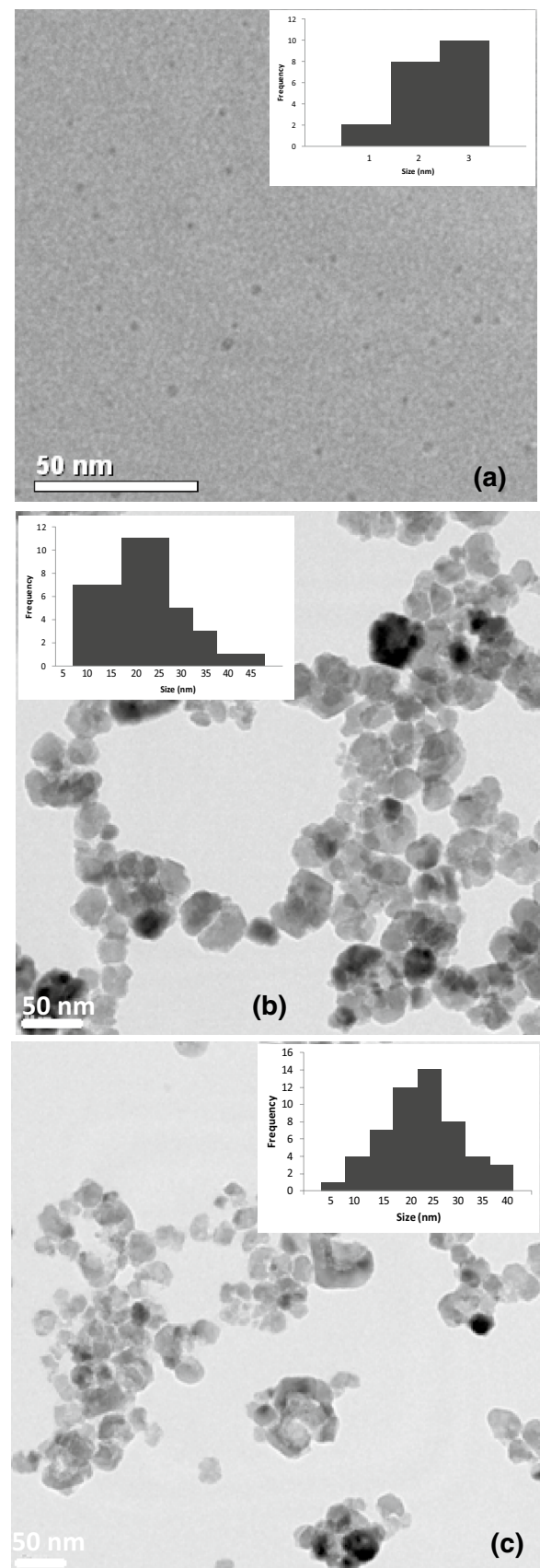
Magnetic measurements of the samples synthesized at different reaction times were made by VSM at room temperature and the hysteresis curves were given in Fig. 8. The  $M_s$ ,  $M_r$ ,  $H_c$  and  $H_s$  values are also given in Table 1. According to the results, sample S1 is not saturated at 20 kOe and the maximum magnetization is 16 emu/g. The  $M_s$  of sample S2 is 47 emu/g and it increases to 57 emu/g for sample S4. The  $M_s$  value is almost constant for the samples S4, S8 and S12 and then increases to 65 emu/g for sample S16. The increase of  $M_s$  may be explained with the increase of particle size as seen in Table 1. The peaks of the secondary phases observed in the XRD patterns of the samples S2 and S4 are quite small (also not observed in the FTIR spectrum) that the magnetic properties are thought to be unaffected by these phases. The  $M_r$  and  $H_c$  of the samples increase whereas the

**Fig. 7** TEM images and histograms of manganese ferrite nanoparticles synthesized at **a** 1 h, **b** 2 h and **c** 16 h

$H_s$  value decreases as the reaction time increases. About 26 nm sized manganese ferrite nanoparticles (S16) show a maximum  $M_s$  value of 65 emu/g with 48 Oe  $H_c$ . The  $M_s$  and  $H_c$  values are significant in accordance with other studies. In the study of Ahmad et al. [10],  $M_s$  and  $H_c$  values of 15 nm sized manganese ferrite nanoparticles synthesized by hydrothermal method are 10 emu/g and 20 Oe, respectively. Haghiri et al. [27] obtained higher  $M_s$  value (52 emu/g) for 9 nm manganese ferrite nanoparticles. For submicron sized (200–400 nm) manganese ferrite spheres, it is shown in [9] that the  $M_s$  is 75 emu/g and  $H_c$  is 12 Oe.

## 4 Conclusions

Manganese ferrite nanoparticles were synthesized by hydrothermal method. The synthesis parameters, reaction temperature and time, were varied separately to investigate the effects of these parameters on the properties of manganese ferrite nanoparticles and optimize the properties of the nanoparticles. X-ray diffraction analysis (XRD), Fourier transform infrared spectroscopy, transmission electron microscopy (TEM) and energy-dispersive X-ray spectroscopy were used to identify and characterize the nanoparticles. The particle sizes were calculated by using the XRD data and TEM images. Physical particle size increases from  $16.1 \pm 6.1$  nm to  $25.8 \pm 7.4$  nm and from  $19.4 \pm 8.4$  nm to  $25.8 \pm 8.2$  nm with the increase of reaction temperature and time, respectively. Magnetic measurements were made by using vibrating sample magnetometer. The saturation magnetization,  $M_s$  was also found to increase with the increase of reaction temperature and time. However, the samples synthesized at high temperature (220 °C) show secondary phase (hematite) in the XRD patterns. Although the  $M_s$  values are very close for the samples synthesized at high temperature (at 220 °C for 4 h) and for long reaction time (16 h at 130 °C), the most appropriate hydrothermal reaction condition to obtain manganese ferrite nanoparticles without other phases was found to be 130 °C and 16 h showing a high  $M_s$  value of 65 emu/g.



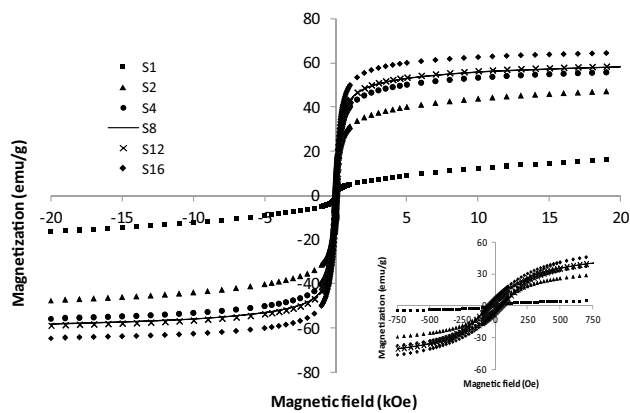


**Fig. 8** Magnetization curves of manganese ferrite nanoparticles synthesized at different reaction times (Inset shows the curves at  $\pm 750$  Oe.)

**Acknowledgements** This work was supported by Balikesir University Research Grant no. BAP 2016/146. The authors would like to thank State Planning Organization, Turkey, under Grant no 2005K120170 for VSM system, Balikesir University, Physics Department for FTIR analysis, Bilkent University, Institute of Material Science and Nanotechnology, UNAM, Turkey, for XRD, TEM and EDX measurements. Authors also thank to H. A. Kargin for the help during synthesis stage.

## References

- B.D. Cullity, *Introduction to Magnetic Materials* (Addison-Wesley Publishing Company, Boston, 1972)
- V. Vignesh, K. Subramani, M. Sathish, R. Navamathavan, *Colloids Surf. A* **538**, 668 (2018)
- S. Kogularasu, M. Akilarasan, S.M. Chen, E. Elaiyappillai, P. Merlin Johnson, T.W. Chen, F.M.A. Al-Hemaid, M.A. Ali, M.S. Elshikh, *Electrochim. Acta* **290**, 533 (2018)
- N. Arsalani, A.G. Tabrizi, L.S. Ghadimi, *J. Mater. Sci.* **29**, 6077 (2018)
- T. Hu, Z. Wang, P. Lv, K. Chen, Z. Ni, *Sens. Actuators B* **266**, 270 (2018)
- N.M. Mahmoodi, *Desal. Water Treat.* **53**, 84 (2015)
- K.W. Jung, S.Y. Lee, Y.J. Lee, *Biores Technol* **261**, 1 (2018)
- T.V. Thu, V.D. Thao, *Appl. Phys. A* **124**, 675 (2018)
- L.X. Yang, F. Wang, Y.F. Meng, Q.H. Tang, Z.Q. Liu, *J. Nanomater.* (2013). <https://doi.org/10.1155/2013/293464>
- A. Ahmad, H. Bae, I. Rhee, *AIP Adv.* **8**, 055019 (2018)
- M. Pernia Leal, S. Rivera-Fernandez, J.M. Franco, D. Pozo, J.M. de la Fuente, M.L. García-Martín, *Nanoscale* **7**(5), 2050–2059 (2015)
- U.I. Tromsdorf, N.C. Bigall, M.G. Kaul, O.T. Bruns, M.S. Nikolic, B. Mollwitz, R.A. Sperling, R. Reimer, H. Hohenberg, W.J. Parak, S. Forster, U. Beisegel, G. Adam, H. Weller, *Nano Lett.* **7**(8), 2422 (2007)
- M.M. Cruz, L.P. Ferreira, J. Ramos, S.G. Mendo, A.F. Alves, M. Godinho, M.D. Carvalho, *J. Alloys Compd.* **703**, 370e (2017)
- Y. Iqbal, H. Bae, I. Rhee, S. Hong, *J. Magn. Mater.* **409**, 80 (2016)
- Z. Chen, X. Sun, Z. Ding, Y. Ma, *J. Mater. Sci. Technol.* **34**, 842 (2018)
- P. Iranmanesh, S. Saeednia, M. Mehran, S. Rashidi Dafeh, *J. Magn. Mater.* **425**, 31 (2017)
- M. Hashim, S.E. Shirsath, S.S. Meena, M.L. Mane, S. Kumar, P. Bhatt, R. Kumar, N.K. Prasad, S.K. Alla, J. Shah, R.K. Kotnala, K.A. Mohammed, E. Şentürk, *J. Alloys Compd.* **642**, 70 (2015)
- A.M. Bolarín-Miró, P. Vera-Serna, F. Sánchez-De Jesús, C.A. Cortés-Escobedo, A. Martínez-Luevanos, *J. Mater. Sci.* **22**, 1046 (2011)
- M. Zahraei, A. Monshi, M.M. del Puerto, D. Shahbazi-Gahrouei, M. Amirnasr, B. Behdadfar, *J. Magn. Mater.* **393**, 429 (2015)
- T. Herranz, S. Rojas, M. Ojeda, F.J. Pérez-Alonso, P. Terreros, K. Pirotta, J.L.G. Fierro, *Chem. Mater.* **18**, 2364 (2006)
- B.D. Cullity, *Elements of X-ray diffraction* (Addison-Wesley, Boston, 1978)
- W. Qin, C. Yang, R. Yi, G. Gao, *J. Nanomater.* **2011**, 159259 (2011)
- J.B. Lee, H.J. Kim, J. Lužnik, A. Jelen, D. Pajić, M. Wencka, Z. Jagličić, A. Meden, J. Dolinšek, *J. Nanomater.* **2014**, 902968 (2014)
- J.L. Rendon, C.J. Serna, *Clay Miner.* **16**, 375 (1981)
- JCPDS card no 10-0319
- JCPDS card no 39-1346
- M.E. Haghiri, A. Izanloo, *Mater. Chem. Phys.* **216**, 265 (2018)
- J.A. Morales-Morales, *Ciencia en Desarrollo* **8**(1), 99 (2017)
- C.P. Hunt, M.B. Moskowitz, S.K. Banerjee, *Magnetic Properties of Rocks and Minerals* (Rock Physics and Phase Relations A Handbook of Physical Constants, American Geophysical Union, Washington, DC, 1995)
- O. Karaagac, H. Kockar, S. Beyaz, T. Tanrisever, *IEEE Trans. Magn.* **46**(12), 3978 (2010)
- F. Ozel, H. Kockar, O. Karaagac, *J. Supercond. Novel. Magn.* **28**, 823 (2015)

**Publisher's Note** Springer Nature remains neutral with regard to jurisdictional claims in published maps and institutional affiliations.